Journal of Advanced Engineering Trends
ISSN : 2682 - 2091

Vol. 44, No. 1, January 2025

Buckling Behavior of Plate Girder with Corrugated Webs Under Shear Load

Sedky A. Tohamy[1], Afaf M. Abdel Halim[1], Fatma Abdel Naser[2], Asmaa Y. Hamed[2,*]

[1] *Civil Engineering Dep., Faculty of Engineering, Minia University, Egypt*
[2] *Construction and Building Dep., The Higher Institute of Engineering and Technology, Luxor, Egypt*
** Corresponding author(s) E-mail: dr_asmaa@adj.aast.edu*

ARTICLE INFO

Article history:
Received: 25 August 2024
Accepted: 29 January 2024
Online: 26 February 2025

Keywords:
Tapered corrugated
Critical shear strength
local buckling
Global buckling
Interactive buckling.

ABSTRACT

Tapered corrugated web (BGCWs) are increasingly being utilized in constructing new bridges due to their lightweight nature, aesthetic appeal, and cost-effectiveness compared to reinforced panels. Existing literature categorizes pointed BGCWs into four distinct typologies, with Case I being the most prevalent and typically found near intermediate abutments in continuous bridges. A parametric study was carried out to investigate the impact of various factors such as the aspect ratio of the web plate, inclination angles of the tapered web plate, web thickness, and fold width. The primary focus of this research is on determining the critical shear buckling stress (τcr) for tapered corrugated web (BGCWs) in Case I through elastic bifurcation analyses using the ABAQUS program on beams with corrugated web subjected to a concentrated load at the mid-span. They found that tapered corrugated web buckling locally, globally, and interactively. Additionally, the study aims to determine the maximum shear load through finite element analysis (FE) to validate the inelastic behavior of tapered BGCWs in Case I. Based on the analysis results, a formula has been proposed to calculate the local ultimate shear force.

1. Introduction

Plate girders are commonly employed to construct industrial structures and bridges. Nevertheless, the use of deep plate girders, which are engineered for extensive spans and substantial loads, can lead to concerns regarding web shear buckling. To address this concern, the integration of stiffener plates can enhance the structural rigidity of slender webs. Furthermore, employing corrugated webs characterized by sinusoidal or trapezoidal geometries can effectively reduce the risk of local buckling while offering a more economical design alternative. It is common practice to select a moderately deep and non-prismatic girder for an efficient design. Despite the advantages offered by plate girders, the susceptibility of their web panels to shear buckling instability due to high panel slenderness ratios is a critical consideration in the design process. Particularly, highway and railroad bridges with thin webs exposed to dynamic loads are at risk of web breathing, which involves recurrent web buckling deformations out of plane. Although extensive research has been conducted on the shear buckling phenomenon for prismatic plates, there is a lack of theoretical and experimental studies on the structural response of tapered steel plate girders under increasing shear loads up to failure.

. This investigation involved an examination of tapered corrugated web to analyze the impact of various factors on shear strength leading up to failure. A novel equation was suggested for determining the maximum shear force during local buckling ($P_{u-Local}$) as there is a lack of experimental and theoretical research on the response of beams with tapered corrugated web to shear stress Various researchers have explored the behavior of beams with taper corrugated webs under shear. Zevallos et al [1] conducted a study on the behavior and shear strength of panel webs in continuous bridges, specifically focusing on Box Girder Concrete Webs (BGCWs) that exhibit tapering near the terminal and intermediate abutments of constructed bridges. Their research involved parametric testing and a comparison with finite element (FE) analysis, revealing that the design model corresponded closely with the actual beams utilized in bridge construction. The research conducted by Shariatyazdi et al [2] involved an experimental analysis of Tapered Cantilever Beams (TCB) that utilized corrugated trapezoidal webs and were subjected to concentrated loads at their terminals. A nonlinear finite element buckling analysis was performed, revealing a strong agreement between the analytical and experimental outcomes. They also formulated a method for calculating the local buckling capacity of TCB, which factors in the influence of the corners of the corrugated web. Shanmugam [3] conducted both experimental and analytical studies to assess the ultimate shear strength of tapered panel girders. The findings indicated that the ABAQUS software is a dependable tool for accurately predicting the ultimate shear strength of these girders. Furthermore, it was noted that the ultimate load capacity of tapered beams surpassed that of straight beams by over 5% when the inclined flanges were subjected to compression. A novel formula was introduced to estimate the ultimate load with adequate precision.

Abdel Aleem et al [4] utilized Multi-Genetic Programming (MGGP) technology to formulate design expressions aimed at predicting the elastic shear buckling strength of tapered end beam

web panels. Their approach demonstrated enhanced prediction accuracy, precision, and consistency compared to existing models. Similarly, Ismail et al [5] harnessed MGGP to explore the nonlinear relationships that dictate the shear behavior of tapered plate girders, successfully establishing dependable predictive expressions for shear strength. Furthermore, Shahin et al [6] implemented an Artificial Neural Network (ANN) methodology to estimate critical elastic buckling coefficients of prismatic tapered steel meshes, achieving superior predictive performance for critical buckling stresses in simply supported tapered prismatic steels subjected to normal and bending forces.

The critical buckling stress is primarily influenced by three factors, namely the aspect ratio ($\alpha = a/h_w$), tapering ratio ($R = h_w/h_1$), and the ratio of minimum to maximum compressive stresses ($\psi = \sigma_2/\sigma_1$), as indicated in the parametric study. Moon et al [7] investigated the lateral-torsional buckling (LTB) of I-girders subjected to uniform bending with corrugated webs. Their results revealed that the flexural strength was predominantly carried by the flanges of these girders. Hamed [8] investigated the impact of shear force on tapered beams with circular and square openings. The numerical findings led to the development of an analytical formula for the critical shear stress of prismatic and tapered mesh panels with circular or square openings. It is important to note that the shear strength can be assessed separately from the moment-shear interaction, thanks to this particular feature. As a result, the average shear stress of the web can be used to compute the constant shear stress Eq (1).

$$\tau = \frac{V}{t_w * h_w} \quad (1)$$

Where V vertical shear force h_w represents the web depth and t_w stands for the web thickness.

2. Problem statement

This study investigates the critical shear stress, proposing an equation to determine the ultimate shear force in the local buckling of tapered corrugated webs. The analysis was conducted using ABAQUS software [9] to carry out elastic bifurcation buckling analyses on tapered corrugated webs in case I as illustrated in Fig. 1. The key aspects of the research involve categorizing the dimensions of the corrugated webs while considering initial imperfections, exploring the failure mode, comparing aspect ratios of different webs, assessing the impact of the inclination α (°) on the load-deformation response, analyzing the influence of web thickness (tw) on critical shear stress, and contrasting analytical results with proposed equations for calculating critical shear force. Moon et al. [7] calculated the critical shear stress in prismatic webs, Hassanein and Kharoob [10] determined the shear stress value in tapered webs, and Shariatyazdi et al. [2] calculated the local buckling coefficient. The findings are presented in Tables 4, 5, and 6. Additionally, the ultimate load value was obtained through nonlinear analysis, and comparisons were made between the results of this analysis and the equations proposed by Sause and Braxtan, as well as Moon et al., as indicated in Table 7.

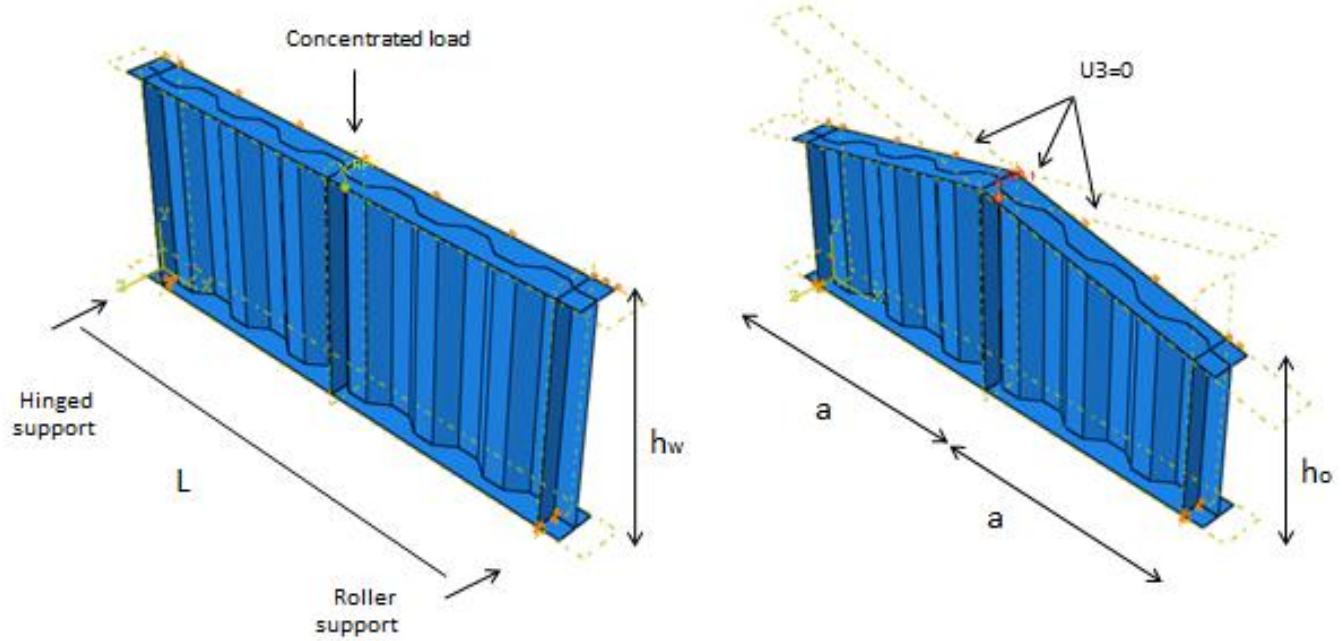

(a) **Prismatic** (b) **Case I**

Figure 1: FE models of tapered BGCWs; (a) prismatic and (b) Case I: Inclined flange under compression & tension field is developed in the short diagonal

3. Finite Element Modeling and Validation

3.1. Input Data

The present study utilized the structural analysis program ABAQUS 6.14 [9] to perform linear and nonlinear buckling analyses aimed at exploring BGCWs featuring a distinct corrugated trapezoidal web configuration. A two-step approach was adopted for the simulation of tapered BGCWs, beginning with an elastic buckling analysis to identify the buckling mode of a flawless BGCW. During the second phase, the adapted RIKS technique was utilized to account for initial geometric defects associated with the first buckling mode in the nonlinear analysis of the BGCW under a concentrated load applied at mid-span. In this analysis, simply supported boundary conditions were implemented, with the left support acting as a hinged support that restricted displacements Ux, Uy, and Uz. The right support, characterized as roller support limited displacements Uy and Uz. Furthermore, to prevent lateral bending and twisting the upper flange was entirely constrained in the Uz direction, as depicted in Figure 1. In the modeling process, the web, flanges, and vertical stiffeners were constructed using the S4R element from the ABAQUS element set. Each node is endowed with three translational and three rotational degrees of freedom, culminating in six degrees of freedom per node. To optimize the mesh, convergence analyses were undertaken. A global element size of 25 mm was determined. The free-type mesh of the finite element model is presented in Figure 2.

3.2. Validation

There is a lack of experimental results in the literature regarding the behavior of tapered BGCWs, despite their practical use. Bedynek et al. [11] conducted tests on tapered plate beams with flat web (B-500-800-1200-3.9-180-15), while Jian et al [12] tested S 1-3. The current Models were validated using available results of prismatic trapezoidal corrugated web beams with constant depths. Table 1 provides comprehensive information on these samples using geometry notations as shown in Fig 3. The results depicted in Fig 4 indicate that the current modeling largely reflects the actual behavior of beams, Girder B, and S 1-3 for the experimental ultimate load. The ratios of (Girder B) and (S 1-3) are 0.97 and1.06, respectively, for (τ_{FE} / τ_{Exp}).

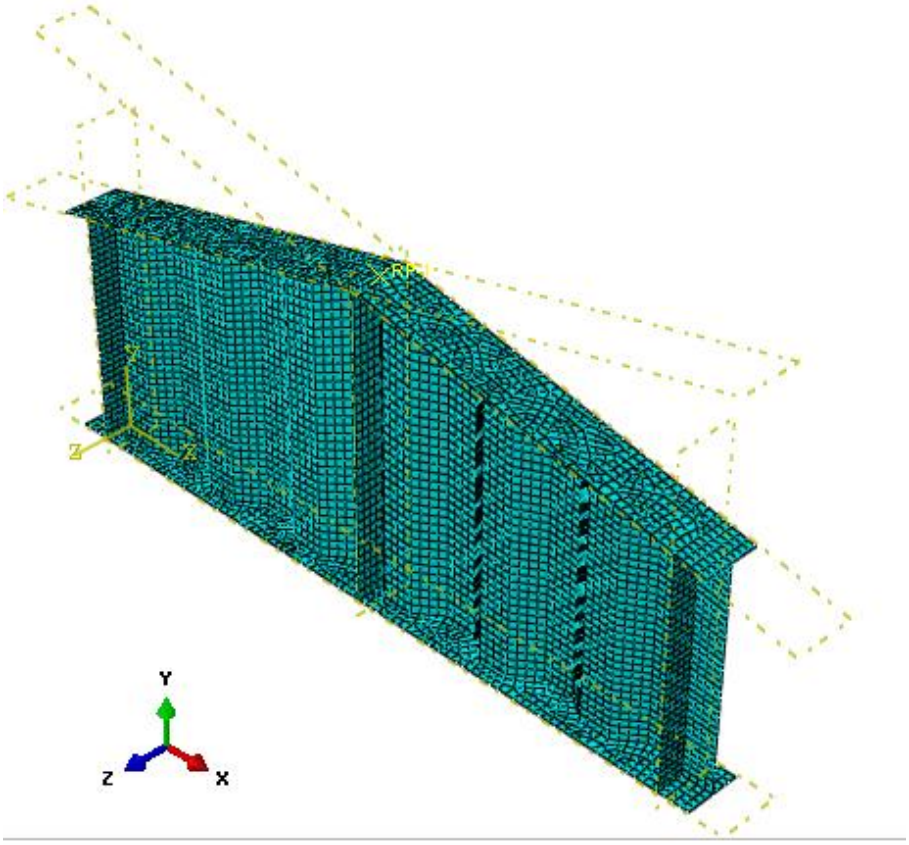

Figure 2: Free type mesh used in the finite element model

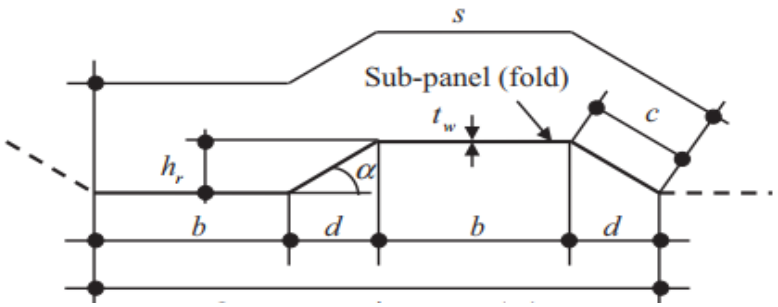

A single wave of corrugation. [13]

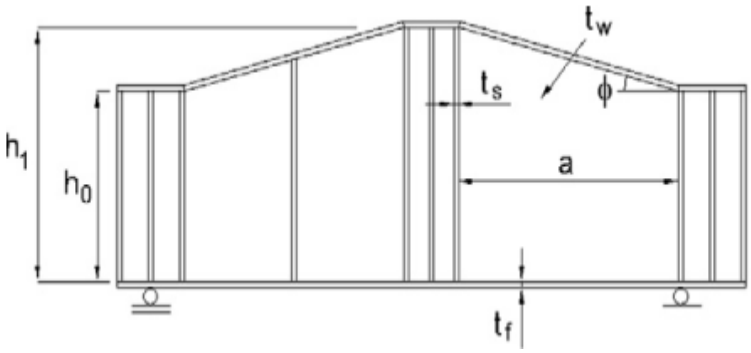

The geometric representations of test girders. [11]

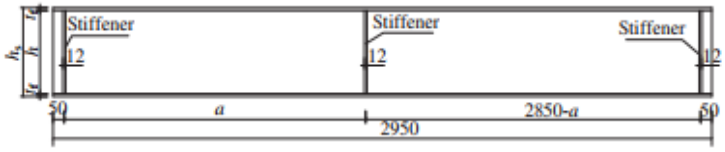

The geometric representations of test girders. (unit: mm)[12].

Figure 3: Types of tested beams

Table 1: Profiles of available tests for Girders

	Tapered Girder	Corrugated Girder
Dim	**B-500-800-1200-3.9-180-15[11]**	**S 1-3[12]**
h_w **(mm)**	**500**	**660**
$h1$ **(mm)**	**800**	**660**
a **(mm)**	**1200**	**1000**
tw **(mm)**	**4**	**0.9**
bf **(mm)**	**180**	**150**
$tf = ts$ **(mm)**	**15**	**14**
an aspect ratio	**1.5**	**1.515**
$tan(\emptyset)$	**0.25**	**-**
fy **(MPa)**	**320.6**	**385.5**
b(mm)	**-**	**20**
d(mm)	**-**	**16**
Θ	**-**	**37**
hr(mm)	**-**	**12**
S(mm)	**-**	**80**
q(mm)	**-**	**72**

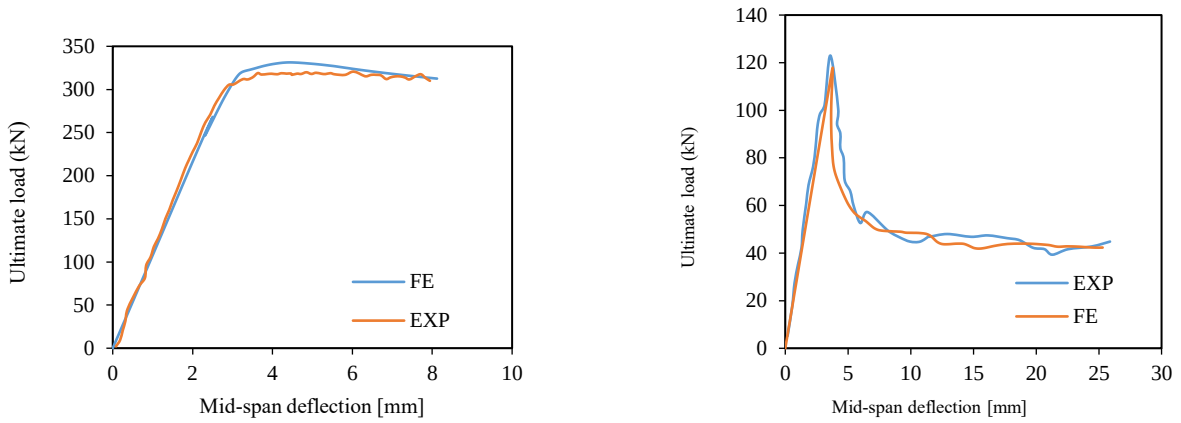

(a) Girder (B) [11] B-500-800-1200-3.9-180-15

(b) S(1-3) [12]

Figure 4: Relationship between ultimate load and mid-span deflection

3.3. . Parametric Study

The study was conducted on BGCWs in the first case using different waviness dimensions. This is a parametric study it was created to compensate for the lack of available design cuts Strengths of tapered BGCWs. Tables 2 and 3 provide details and dimensions FE for tapered BGCWs with case I. The thickness of the web ranges between 2 and 4 mm. Primary geometric defects, based on the first positive shear the buckling mode was included in the nonlinear analysis of BGCW with values of $(L/1000)$. Simply supported conditions were applied to the end sections. It has steel material it is modeled as a von Mises material with isotropic hardening. The steel used was S355 according to EN 1993-1-1 [14], which it has a steel yield (fy) and ultimate strength (fu) of 355 MPa and 510 MPa respectively. Currently, 3D FE models, using ABAQUS [9] FE. The package was implemented on one hundred and twenty, including thirty prismatic beams and ninety tapered BGCWs. This covers the following parameters:

- Aspect ratio of web panels $(a\ /\ h_{w1})$ = (1, 1.2 and 1.5).
- Inclination flange angle α ° = (0, 5, 10, 15).
- Web thickness (t_w) = (2, 3 and 4 mm).
- Fold width (b) = (10, 50, 100, and 150).

The structure of each girder consisted of a corrugated web accompanied by two flat, compact flanges. To meet the design criteria, the flat flanges were designed with a width of 180 mm and a thickness of 15 mm, thereby satisfying the condition that the ratio of flange thickness to web thickness $(tf/tw \geq 3.0)$. Corrugation specifications for the parametric study, four groups of BGCWs were designed. The first group had a fold width of 10 mm, while the second, third, and fourth groups were 50, 100, and 150 mm, respectively, and the inclination angle was (37°) as shown in Table 1. For each group, BGCWs have a different taper angle α (°), 0, 5, 10, and 15. The prismatic girder's web depth was 1000 mm, equivalent to the tapered girders' dimension $(hw1)$. Hence, the web panel's aspect ratio (a/hw) was (1, 1.2and 1.5), in which the distance between its vertical stiffeners is greater or equal to the web's depth (hw) as shown in Table 3.

Table 2: Corrugated steel web profiles and their geometric characteristics.

Name	b(mm)	d = c = w (mm)	h_r(mm)		S(mm)	q(mm)	Ø(°)
I-A-10	10	8	6.02		40	36	37
I-A-50	50	40	30.08		200	180	37
I-A-100	100	80	60.16		400	360	37
I-A-150	150	120	90		600	540	37

Table 3 Details of the FE program.

Name	a/h	hw(mm)	Typology	b(mm)	α (°)	t_w(mm)	No. of models
I-A	1	1000	Prismatic	10,50,100,150	0.0	2,3,4	12
I-A	1	1000	Case I	10,50,100,150	5,10,15	2,3,4	36
I-B	1.2	1000	Prismatic	50,100,150	0.0	2,3,4	9
I-B	1.2	1000	Case I	50,100,150	5,10,15	2,3,4	27
I-C	1.5	1000	Prismatic	50,100,150	0.0	2,3,4	9
I-C	1.5	1000	Case I	50,100,150	5,10,15	2,3,4	27
Total no. of models							120

4. Results and discussions

The evaluation of the critical shear stress ($\tau cr.FE$) associated with a particular model, regardless of its mode of buckling, is a direct consequence of the elastic bifurcation buckling analyses that have been executed. Therefore, the results of these analyses are presented in the following section

4.1. Modes of buckling

The previously referenced FE program was employed to derive three separate modes in corrugated webs by adjusting the widths of the web folds. The prismatic and tapered corrugated web configurations depicted in Figure 5 represent the local, interactive, and global buckling modes relevant to case I. Within a single sub-panel (fold) of the web, the occurrence of deformations plays a crucial role in determining the local buckling mode, especially in instances where the fold widths are considerable. In contrast, the global buckling mode is characterized by multiple folds, with the buckled configuration intersecting the depth of the web diagonally. the interactive buckling mode appears to fuse characteristics of both the global and local buckling modes. The buckling patterns generated by the tapered webs were consistent with those of prismatic webs. In contrast, the local and interaction buckling waves associated with the tapered plates were primarily displaced towards their shorter vertical ends. For both undulations, the interactive buckling mode was observed where the fold width was 50,100 mm, and the global buckling was observed for the fold widths of 10 and 50 mm. While the local buckling was for the fold width of 100,150 mm in this case, the type of buckling depends on the thickness of the web to some extent.

4.2. Effects of tapered web typology

The analysis of various tapered corrugated webs, which share the same geometry as the buckling behavior of prismatic beams, demonstrated differences in the values of critical shear stress ($\tau cr.FE$). The normalized critical stresses for different typologies were determined using a prismatic web characterized by uniform web thickness and fold width, as demonstrated in Figure 6.The figure demonstrates that ($\tau_{cr.FE}$) is lower than the prismatic lattice value for (a/h) ratios of 1, 1.2, and 1.5. Moreover, it was observed that ($\tau_{cr,FE}$) decreases with increasing (a/h) ratio and inclination angle α (°). This suggests that the (τ_{cr}) value predictions for tapered webs, when calculated using prismatic web data, may lead to overestimations. Furthermore, the figure indicates that increasing web thickness results in higher normal critical stresses for different types, except for ($a/h = 1.5$) where conservative values are provided. Notably, ($a/h = 1.0$) yields the most accurate estimate of critical pressures.

4.3. *Effects of inclination angle*

It was observed that the inclination angle α (°) affects critical shear stresses($\tau\_(cr.FE)$). Fig. 8 shows the relationship between the critical shear stress of tapered webs for those of prismatic gratings ($\tau\_(cr.FE)/\tau\_(cr.Prop)$) and inclination angle α (°). For beams with web thickness tw = 2 mm and fold widths b = 150 mm, as can be Observed, increasing the value of α (°) reduces the values of ($\tau\_(cr.FE)/\tau\_(cr.Prop)$), Fig (7- a). On the other hand, for beams with web thickness $tw = 2$ mm and fold width b = 100 mm at angle α. (5°) increases the value of ($\tau\_(cr.FE)/\tau\_(cr.Prop)$) and becomes greater than one, and conclude that when b = 100 mm it gives better results than when α (5°) Fig (7).

4.4. Effects of web thickness

The thickness of corrugated webs increases the patterns and excites the critical shear stress($\tau_{cr.FE}$). As shown in Fig. 8,this Figure shows the relationship between ($\tau_{cr.FE}$) and web thickness when $b = 50$ mm, $b = 100$ mm. As can be seen, the increase in ($\tau_{cr.FE}$) it is made approximately linear by increasing the thickness of the tapered corrugated web. As can be seen, by increasing the value of α (°), the value of ($\tau_{cr.FE}$) increases.

4.5. Evaluations of existing buckling stress values.

4.5.1 Prismatic corrugated webs

This section compares the available critical stresses recommended by Moon et al. [15] with the critical shear values of the prismatic webs ($\tau_{cr,\ FE,\ P}$) For the following cases, Local shear buckling ($\tau_{cr,l}$) Eq(2), Global shear buckling ($\tau_{cr,\ G}$) Eq (3-4) and Interactive shear buckling ($\tau_{cr\ I}$) Eq(5-6). used local shear buckling coefficient (k_l) with the value of 5.34 [15] Comparison results are provided in Table (4). It is evident from the comparative findings that the local buckling strength is suitable for the condition of corrugated web proposed by Moon et al [15] both three values (a/h=1, 1.2, 1.5), However, it give unsafe results in global and interactive shear buckling.

$$\tau_{\mathrm{cr.l}} = k_l \frac{\pi^2 E}{12(1-v^2)\left({}^{w}/_{t_w}\right)^2} \tag{2}$$

$$\tau_{cr.G} = k_G \frac{\pi^2 E}{12(1-v^2)} \left(\frac{t_w}{h_w}\right)^2 \tag{3}$$

$$k_G = 5.72 \left(\frac{d}{t_w}\right)^{1.5} \tag{4}$$

$$\tau_{cr.I} = k_I \frac{\pi^2 E}{12(1-v^2)} \left(\frac{t_w}{h_w}\right)^2 \tag{5}$$

$$k_I = \frac{30.54}{5.34\left(\frac{d}{t_w}\right)^{-1.5} + 5.72\left(\frac{w}{t_w}\right)^2} \tag{6}$$

4-5-2 Tapered corrugated webs

The critical shear values for The tapered web ($\tau_{cr,\ FE}$) are compared with the equations proposed by Hassanein and Kharoob [10]. Eq (7), from the comparison results, it can be noted that the critical buckling strength is suitable for the case of corrugated web with a value of a/h = 1, α (°) = 5, and that it gives unsafe results in other cases, as shown in Table (5). The tapered web was also compared with the equation proposed by Payam Shariatyazdi et al. [2]. Eq (8, 9), in the case of local buckling strength, and from the comparison results, it was noted that it gives suitable results in the case of a/h = 1, w/tw > 50, and unsafe results in the other cases Shown in Table (5).

$$\tau_{cr.mf} = {\tau_{cr.FE.P}}/{(1+\tan\alpha)} \text{ for Case I} \quad (7)$$

$$\tau_l = k_l \frac{\pi^2 E}{12(1-\upsilon^2)} \left(\frac{t_w}{w}\right)^2 \quad (8)$$

$$k_l = 6.81 - 45.47\frac{1}{\theta} + 2.21\left(\frac{w}{h}\right) + 4.37\left(\frac{w}{h}\right)^2 + 45.25\frac{\left(\frac{w}{h}\right)}{\theta} \quad (9)$$

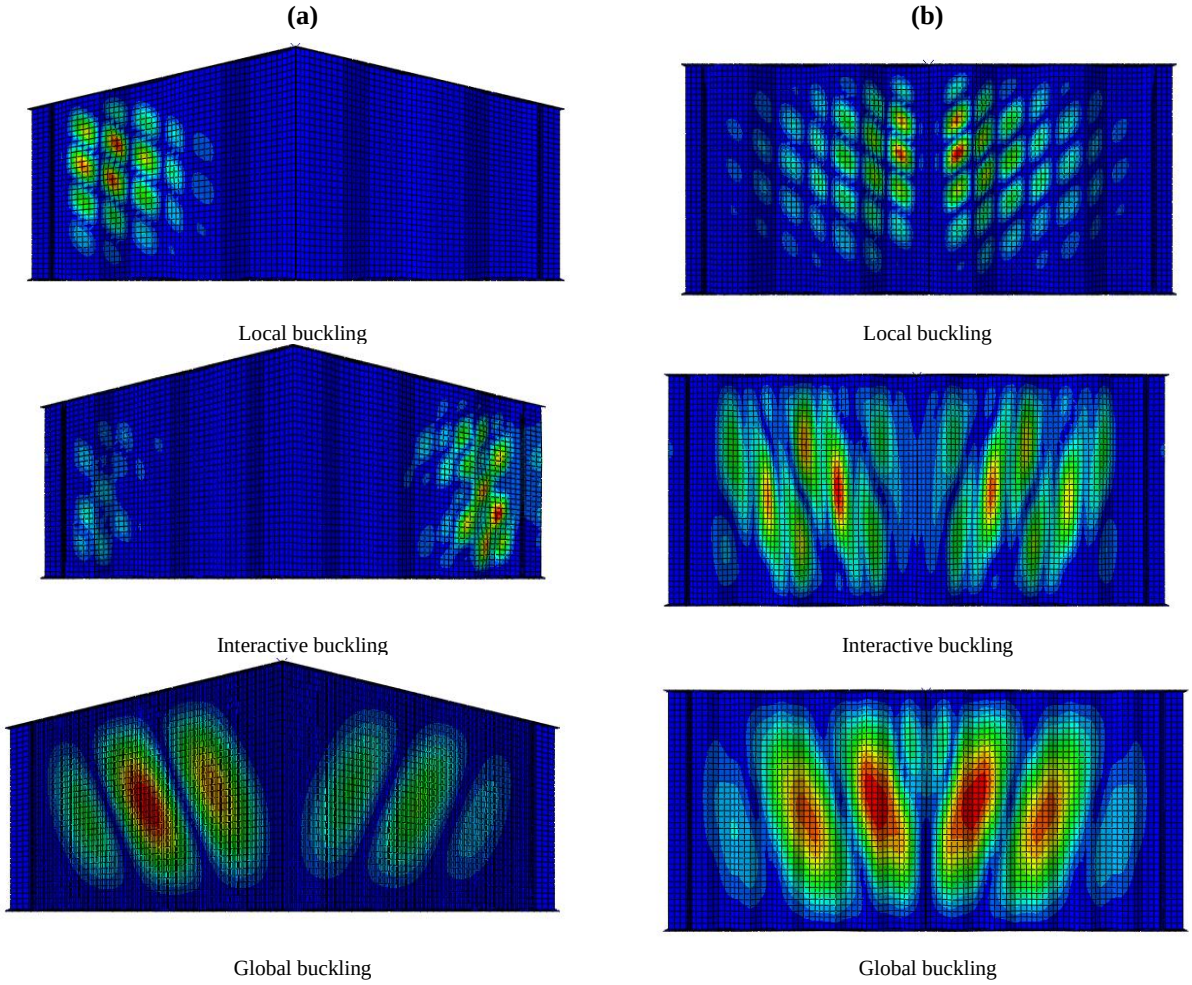

Figure 5: Different buckling modes in (a) tapered corrugated webs and (b) prismatic

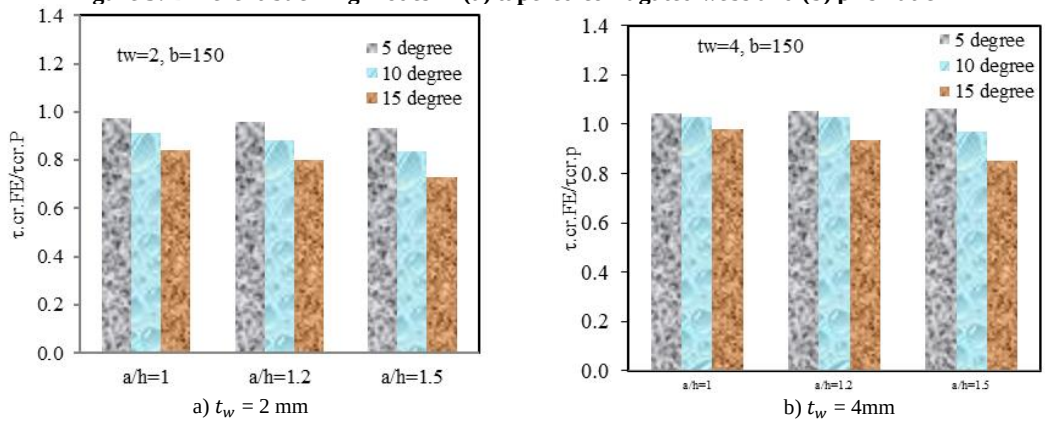

a) t_w = 2 mm b) t_w = 4mm

Figure 6: The normalized critical stresses for tapered corrugated webs are as follows: (a) t_w = 2 mm and (b) t_w = 4mm

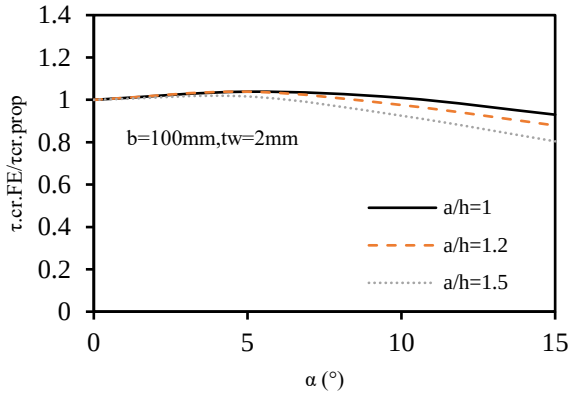

(a) b = 100mm

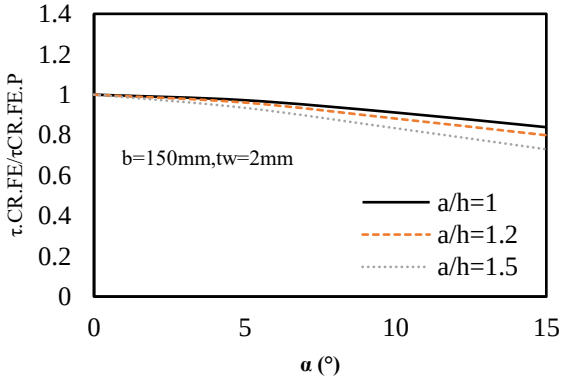

(b) b = 150mm

Figure 7: Relationship between normalized critical stresses and inclination angle

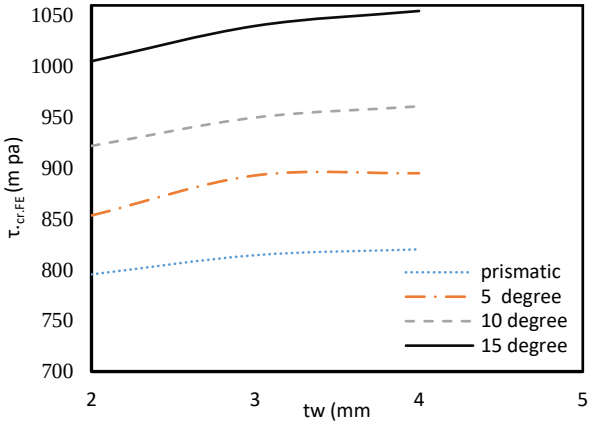

(a) b = 50 mm

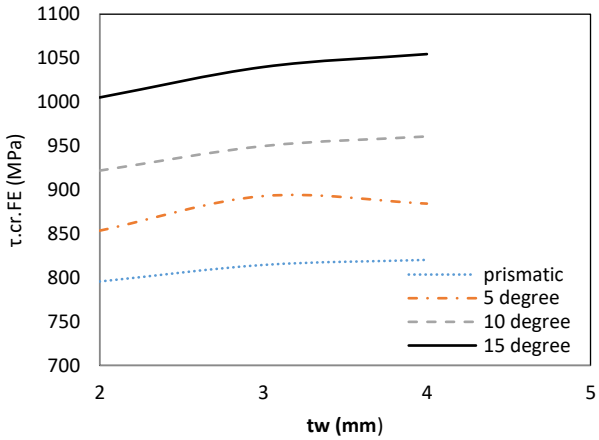

(b) b = 100 mm

Figure 8: FE critical stresses for tapered corrugated webs with: (a) b = 50, (b) b = 100 m

Table 4: An analysis of the critical shear stress ($\tau_{cr.prop}$) associated with prismatic corrugated webs is presented

Girder						
Case I-a/h=1-b-tw-α (°)	$a/h = 1.0$		$a/h = 1.2$		$a/h = 1.5$	
	Buckling mode	$\tau cr.FE / \tau cr.Eq$	Buckling mode	$\tau cr.FE / \tau cr.Eq$	Buckling mode	$\tau cr.FE / \tau cr.Eq$
I-A-1-10-2-0	G	1.32	-	-	-	-
I-A-2-50-2-0	G	2.05	I	2.53	I	2.50
I-A-3-100-2-0	L	1.21	L	1.20	L	1.20
I-A-37-150-2-0	L	1.18	L	1.18	L	1.18
I-A-4-10-3-0	G	1.45	-	-	-	-
I-A-5-50-3-0	G	1.72	G	1.68	G	1.64
I-A-6-100-3-0	I	1.46	I	1.45	I	1.44
I-A-38-150-3-0	L	1.05	L	1.05	L	1.05
I-A-7-10-4-0	G	1.62	-	-	-	-
I-A-8-50-4-0	G	1.50	G	1.83	G	1.41
I-A-9-100-4-0	I	1.38	I	1.37	I	1.36
I-A-39-150-4-0	L	0.92	L	0.92	L	0.92
Ave		1.41		1.47		1.41

Table 5: Comparison between the critical shear stress ($\tau_{cr, FE}$) of the taper corrugated webs ([10] [2])

GIRDER	Hassanein And Kharoob[11]			Shariatyazdi Et Al.[2]			
	$\tau_{cr, FE}/\tau_{cr, Eq}$			$\tau_{cr, FE}/\tau_{cr, Eq}$			w/tw
	a/h=1	a/h=1.2	a/h=1.5	a/h=1	a/h=1.2	a/h=1.5	75
I-150-2-5	1.06	1.04	1.02	0.99	0.98	0.95	50
I-150-3-5	1.12	1.12	1.09	0.94	0.93	0.91	37.5
I-150-4-5	1.14	1.15	1.09	0.83	0.84	-	50
I-100-2-10	1.19	1.15	0.98	1.09	1.05	1.00	75
I-150-2-10	1.07	1.04	1.06	0.93	0.90	0.85	50
I-150-3-10	1.15	1.12	1.14	0.89	0.86	0.81	37.5
I-100-2-15	1.18	1.21	1.02	1.00	0.95	0.87	75
I-150-2-15	1.06	1.11	0.92	0.85	0.81	0.74	50
I-150-3-15	1.15	1.01	0.99	0.82	0.78	0.71	37.5
I-150-4-15	1.24	1.09	1.08	0.78	0.74	0.67	75
NOTE: CASE I-B-TW-A (°)							

5. Nonlinear buckling analysis

5.1. Results and discussions

The findings from the current nonlinear buckling analyses encompass various failure modes, the relationship between load and mid-span deflection, and the ultimate shear force ($Pul.FE$). The Shear buckling coefficient for corrugated web configurations $\lambda_s = \sqrt{\tau_y/\tau_I}$) was determined; $\tau\, I$ was determined for each type using Eq. (7). As indicated by Table (7) λ_s is greater than 1 for BGCWs. The prismatic and tapered cases were considered with tw = 4 mm, angle 5°, and ratio a/h = (1, 1.2, 1.5) for the tapered beams. Fold width of 50 To 150 mm in increments of 50 mm. This resulted in twelve prismatic and twelve tapered BGCWs. These are the FE results in Table 7. Eq. (1) was used to determine peak shear stress values ($\tau ul.FE$) at the critical cross-section of the BGCWs in all situations, using the shorter web dimension (hwo). The relative values of τul and the $\tau ul.FE\ /\tau y$ ratio were also calculated, with τy as the yield shear strength of the base material and ($\tau_y = f_y/\sqrt{3}$). Except for the girder of Case (I) with $tw = 4\,mm.b = 150\,mm$ which failed due to flange yielding (flexural failure (F)), All full-scale BGCWs were tested under shear loading conditions until they reached failure. Local (L), interactive (I), and global (G) shear buckling failure modes appeared. Table 7 shows that local shear buckling was associated with BGCWs with high (b) values, while interactive shear buckling mode was evident in beams with relatively high (b) values. Simultaneously, the manifestation of global shear buckling was noticeable in beams possessing reduced (b) values. The transition from general mode to reactive mode involves the presence of prismatic beams. This indicates that the tapered BGCW may alter its failure mode. The stress distribution at ultimate shear loads for prismatic and tapered beams is depicted in Figure 9. Areas that demonstrate strength greater than the yield strength of the material are marked with a red tint. These regions are focused on the side exhibiting the highest shear stress, which pertains to the short depth of the webs (hwo). Each shear span (a) resulted in the formation of nearly one corrugation wave. Table 7 illustrates that the ultimate shear force ($Pul.FE$) of the BGCWs is consistently greater for tapered girders compared to prismatic girders. Notably, the highest $Pul.FE$ values occur when the aspect ratio a/h is equal to 1. In contrast, the scenarios with aspect ratios of a/h equal to 1.2 and 1.5 yield comparatively lower $Pul.FE$ results. On the other hand, Cases I ($\tau ul.FE/\tau y$) show values approaching unity, as depicted in Fig 10. This suggests that the materials can be utilized effectively. Additionally, a rise in the tw value leads to a linear increase in the strengths of the BGCWs, which is evident in Fig. 11. It can also be noted that increasing the value of α reduces the strengths. Fig 12 shows an example of the load-mid-span deflection for the BGCWs. Here, Case I (α=15°) was used as an example. It is evident that the failure is abrupt and stems from buckling for the big (i.e., 150 = b mm) BGCW of fold width. In tapered BGCWs with a b value of 10 mm, the transition from the pre-peak to the post-peak stages occurs smoothly.

5.2. Comparisons with available shear strengths

The shear strengths for prismatic BGCWs proposed by Moon et al. [15] Eq. (10) and Sause and Braxtan [16] Eq. (11) were compared to the final strengths of the current models. This was created by substituting the corrugated webs' current shear buckling parameter $\lambda_s = \sqrt{\tau_y/\tau_I}$) for their parameters. The results are provided in Table 6. The shear strength of Moon et al. [15] provides unconservative predictions for prismatic and tapered girder. [15] may be used by reducing it ($\tau_{ul,\,M,\,mod}$) by the ratio hwo/hw1 In case I as previously suggested by Bedynek et al. [11]; see Table 7., while that predicted by Sause and Braxtan [16] is conservative. On the other hand, the $\tau_{ul,s}$ values according to Sause and Braxtan [16] provide accurate and better estimates for the Prismatic girder.

$$\frac{\tau_{ul.m}}{\tau_y} = \begin{cases} 1 : \lambda_s < 0.6. \\ 1 - 0.614(\lambda_s - 0.6) : 0.6 \le \lambda_s < \sqrt{2} \\ 1/\lambda_s{}^2 : \lambda_s \ge \sqrt{2} \end{cases} \tag{11}$$

$$\frac{\tau_{ul.s}}{\tau_y} = \tau_y \left(\frac{1}{(\lambda_s)^6+2}\right)^{\frac{1}{3}} \tag{12}$$

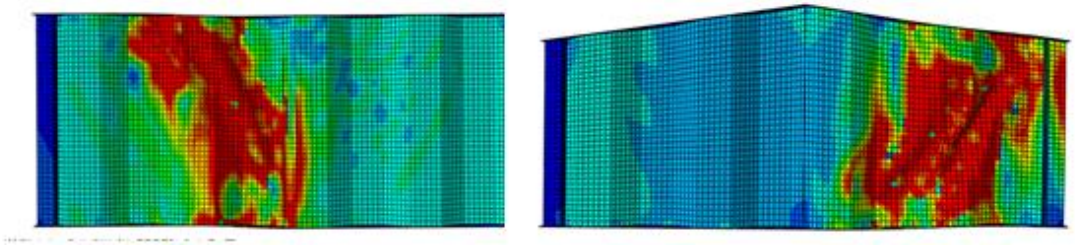

(a) Prismatic (b) Case I

Figure 9: Stress profile analysis of BGCWs with a 10 mm web thickness

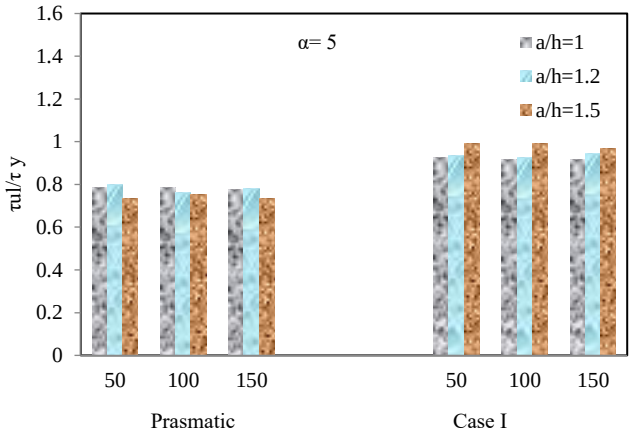

Figure 10: A study contrasting τul and $FE/\tau y$ ratios for different categories

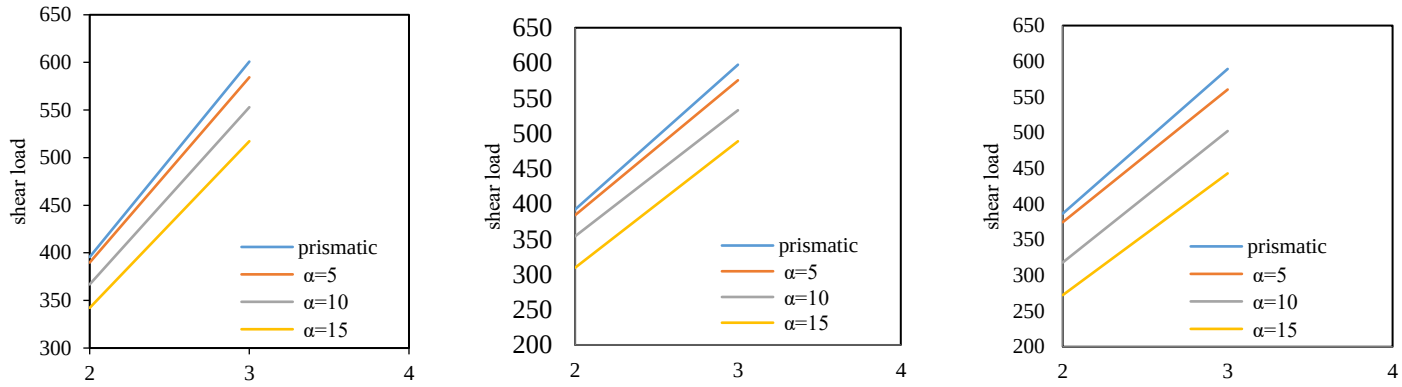

(a) $(^{a}/_{h} = 1)$ **(b)** $(^{a}/_{h} = 1.2)$ **(c)** $(^{a}/_{h} = 1.5)$

Figure 11: Comparative study of shear ultimate strengths by web thickness among classifications

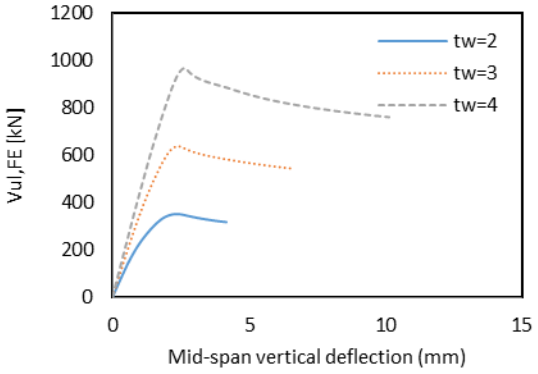

(a) b =10mm

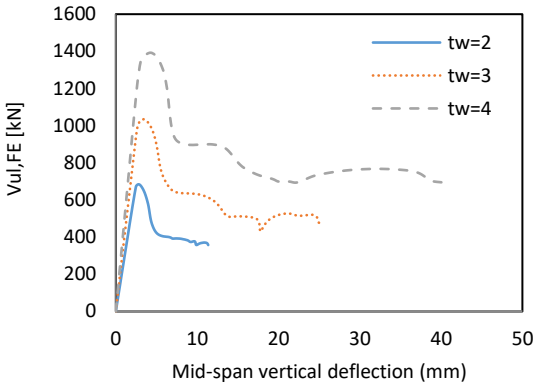

(b) b =50mm

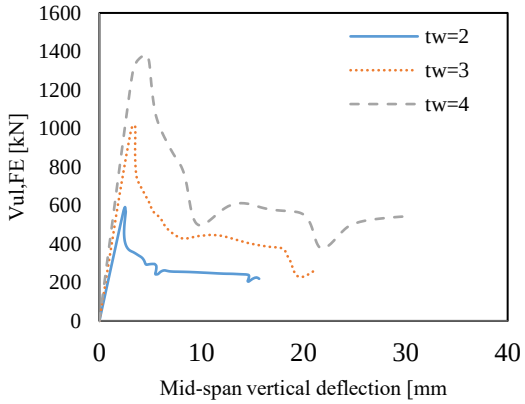

(c) b =100mm

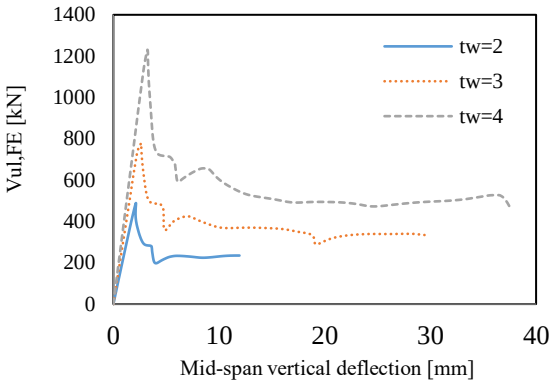

(d) b =150mm

Figure 12: The ultimate shear strengths and the mid-span vertical deflection for Case I, where $\alpha = 15$

Table 6: FEM Results

Type	(a/h)	b(mm)	λs	P_{ul-FE} [kN]	Buckling mode	$\tau ul.FE$ [MPa]	$\tau ul.FE/\tau y$	$\tau ul;\ M/\tau y$	$\tau ul;S/\tau y$
Prismatic	1	50	1.13	654	G	163.42	0.79	0.99	0.78
		100	1.13	654	I	163.40	0.79	1.00	0.79
		150	1.13	646	L	161.58	0.78	1.00	0.79
Case I		50	1.18	702	I	192.32	0.93	0.97	0.78
		100	1.18	696	I	190.75	0.92	1.00	0.79
		150	1.18	697	F	190.94	0.92	1.00	0.79
Prismatic	1.2	50	1.12	665	G	166.24	0.80	0.99	0.78
		100	1.14	636	I	158.88	0.76	1.00	0.79
		150	1.13	649	L	162.14	0.78	1.00	0.79
Case I		50	1.17	695	G	193.98	0.93	0.99	0.79
		100	1.19	690	I	192.67	0.93	1.00	0.79
		150	1.18	704	F	196.76	0.95	1.00	0.79
Prismatic	1.5	50	1.17	612	G	153.05	0.74	0.99	0.78
		100	1.15	624	I	156.06	0.75	1.00	0.79
		150	1.17	609	L	152.17	0.73	1.00	0.79
Case I		50	1.22	668	G	192.30	0.93	0.99	0.79
		100	1.20	685	I	197.14	0.95	1.00	0.79
		150	1.22	652	F	187.66	0.90	1.00	0.79

Table 7: Suggested strengths for tapered BGCWs of Cases I

Type	a/h	b (mm)	λs	$Vul.FE$ [kN]	Buckling mode	$\tau ul.FE$ [MPa]	$\tau ul.FE$ / τy	$\tau ul.M.mod$ /τy
Case I	1	50	1.18	702	I	192.32	0.93	0.89
		100	1.18	696	I	190.75	0.92	0.91
		150	1.18	697	F	190.94	0.92	0.91
Case I	1.2	50	1.17	695	G	193.98	0.93	0.89
		100	1.19	690	I	192.67	0.93	0.90
		150	1.18	704	F	196.76	0.95	0.90
Case I	1.5	50	1.22	668	G	192.30	0.93	0.86
		100	1.20	685	I	197.14	0.95	0.87
		150	1.22	652	F	187.66	0.90	0.87

5.3. proposed formula

In this research, an equation was deduced through the results obtained from finite element analysis to calculate the ultimate shear force in the case of local buckling ($P_{ul,\ l}$) through four variables:

- X_1 (a /h) is a variable that gives a quadratic equation.
- X_2 (tw) is a variable that gives a quadratic equation.
- $X_3(\alpha^{\circ})$ is a variable that gives a third-degree equation.
- X_4 (b) is a variable that gives a first-degree equation.
- y (P_{ul}) is a dependent variable

The variables were collected in the Eq (12), and using the SPSS program for multivariate regression analysis, the constant coefficients (a, a1, a2, a3, a4, a5, a6, a7 a8) were obtained by determining the constant Parameterizing the results of finite element models the e Eq (13) becomes as follows:

$$y = a + a_1x_1 + a_2{x_1}^2 + a_3x_2 + a_4{x_2}^2 + a_5x_3 + a_6{x_3}^2 + a_7{x_3}^3 + a_8x_4 \quad (12)$$

$$P_{ul,l} = -140.85 + 180.27(\frac{a}{h}) - 180.06\left(\frac{a}{h}\right)^2 + 323.31(t_w) - 24.61(t_w)^2 + 0.122(\alpha) - 0.797\alpha^2 + 0.026\alpha^3 - 1.12b \quad (13)$$

where R-squared was its value of 0.956 fits well with the results obtained from the finite element analysis of the models. Where (Pul) ultimate shear strength, (a/h) Aspect ratio of web panels, (tw) web thickness, (α°) Inclination flange angle, and (b) fold width. It can be noted that the proposed local shear strength value is consistent with the shear strength value resulting from the finite element analysis. Figure (13) provides the proposed local ultimate shear force ($Pul.l.Prop$) to the local ultimate shear force in FE ($Pul.l.FE$). As can be seen, the above equations can effectively It can be used to predict the local ultimate shear strength of tapered corrugated web, provided that it is within the following limits: the slenderness ratio (hw/tw) ranges from 250 to 500, the fold width to height ratio (b/hw) is from 0 1. 0.15, the inclination angle (α°) is from 0 to 20, and the aspect ratio to the web panel (a/hw) is from 1 to 1.5.

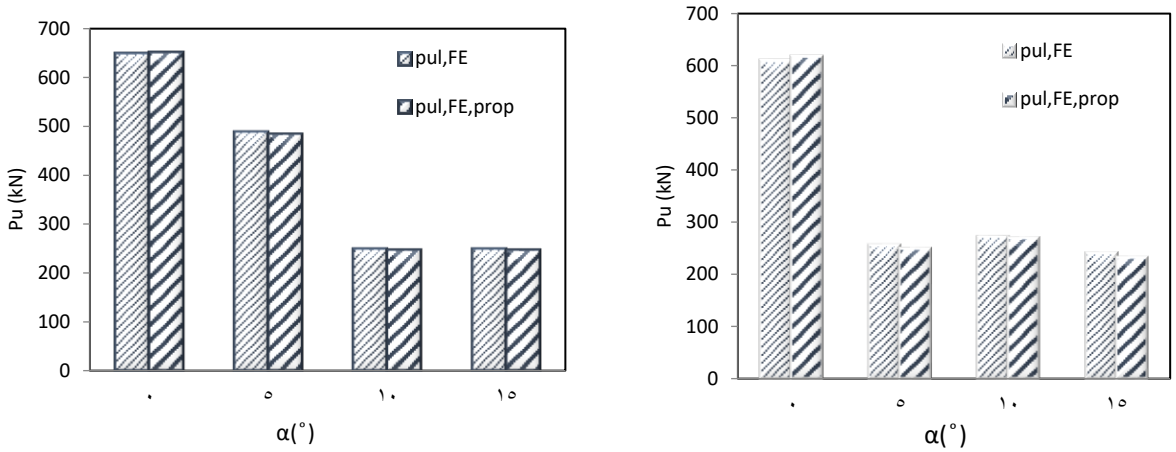

(a) (a/h)=1.2 (a/h)=1.5

Figure 13: Comparison of $P_{ul.FE}$. $P_{ul.FE.prop}$ with different ratios a/h

6. Summary and Conclusions

It was observed that the prediction value of $\tau_{cr.FE}$ for tapered web, when calculated using prismatic web data, may lead to overestimation. On the other hand, the value of $\tau_{cr.FE}$ is lower than that of the prismatic web for ratios $(a\ /\ h)$ 1, 1.2, and 1.5. Moreover, it was observed that $\tau_{cr.FE}$ decreases with increasing (a/h) ratio and inclination angle α (°).

Increasing angle α (°) decreases the values of $\tau_{cr.FE}/\tau_{cr.prop}$ whereas for beams at angle α (5°) with web thickness $tw = 2\,mm$ and fold width $b = 100\,mm$, the values of $\tau_{cr.FE}/\tau_{cr.prop}$ increase and become greater than one, indicating that $b = 100\,mm$ produces better results than when α (5°).

There is a linear relationship between the critical stress $\tau_{cr.\ FE}$ and web thickness, meaning that the higher the web thickness, the critical stress $\tau_{cr.FE}$.

By comparing the available critical pressures recommended by Moon et al. [15], with the critical shear values for prismatic web $\tau_{cr.FE.p}$ it is clear from the comparative results that the local buckling strength is suitable for the case of corrugated fabric proposed by Moon et al. [15] Both three values (a/h = 1, 1.2, and 1.5) However, it gives unsafe results in global and interactive shear buckling.

By comparing the available critical stresses proposed by Hassanein and Kharoob [10] with the critical shear values for tapered webs ($\tau cr.FE$), it is clear from the comparative results that the critical buckling force is suitable for the case of corrugated fabric with a value of $a/h = 1$, α (°) $= 5$. It is unsafe and results in other conditions. On the other hand, the results were also compared to the available critical pressures proposed by Payam Shariatyazdi et al. [2]. From the comparison results, it was noted that it gives suitable results in the case of $a/h = 1$, $w/tw > 50$ and unsafe results in the case of other cases.

Tapered beams always have higher Pul. FE values than prismatic values. However, a higher value of Pul, FE was found in Case $a/h = 1$. the two cases $a/h = (1.2.\text{and } 1.5)$ give lowers results.

From the results of the comparison between the ultimate strength of existing models and the prismatic shear force proposed by Moon et al. [15] it was unconservative for prismatic and tapered beams. While it gives safe results if $\tau_{ul.m,mod}$ is reduced by $hwo/hw1$, On the other hand, the values of τul. s according to Sause and Braxtan [16] provide accurate estimates ideal for the prismatic model.

Proposed local shear strength $P_{ul.1.FE}$ value is consistent with the shear strength value resulting from finite element analysis

References

[1] E. Zevallos, M. F. Hassanein, E. Real, and E. Mirambell, "Shear evaluation of tapered bridge girder panels with steel corrugated webs near the supports of continuous bridges," *Eng. Struct.*, vol. 113, pp. 149–159, Apr. 2016, doi: 10.1016/j.engstruct.2016.01.030.

[2] P. Shariatyazdi, H. Ronagh, M. Izadinia, and M. R. Javaheritafti, "Shear buckling behavior of tapered cantilever beams with corrugated trapezoidal web under concentrated tip load," *J. Constr. Steel Res.*, vol. 193, no. April, p. 107265, 2022, doi: 10.1016/j.jcsr.2022.107265.

[3] N. E. Shanmugarr and H. Min, "Ultimate load behaviour of tapered steel plate girders," *Steel Compos. Struct.*, vol. 7, no. 6, pp. 469–486, 2007, doi: 10.12989/scs.2007.7.6.469.

[4] B. H. AbdelAleem, M. K. Ismail, M. Haggag, W. El-Dakhakhni, and A. A. A. Hassan, "Interpretable soft computing predictions of elastic shear buckling in tapered steel plate girders," *Thin-Walled Struct.*, vol. 176, Jul. 2022, doi: 10.1016/j.tws.2022.109313.

[5] M. K. Ismail, B. H. AbdelAleem, A. A. A. Hassan, and W. El-Dakhakhni, “Prediction of tapered steel plate girders shear strength using multigene genetic programming,” *Eng. Struct.*, vol. 295, no. September, p. 116806, 2023, doi: 10.1016/j.engstruct.2023.116806.

[6] R. I. Shahin, M. Ahmed, S. A. Yehia, and Q. Q. Liang, “ANN model for predicting the elastic critical buckling coefficients of prismatic tapered steel web plates under stress gradients,” *Eng. Struct.*, vol. 294, no. July, p. 116794, 2023, doi: 10.1016/j.engstruct.2023.116794.

[7] J. Moon, J. W. Yi, B. H. Choi, and H. E. Lee, “Lateral-torsional buckling of I-girder with corrugated webs under uniform bending,” *Thin-Walled Struct.*, vol. 47, no. 1, pp. 21–30, 2009, doi: 10.1016/j.tws.2008.04.005.

[8] A. Hamed, “ELASTIC SHEAR BUCKLING OF Tapered STEEL PLATE GIRDERS with OPENING IN WEB,” *JES. J. Eng. Sci.*, vol. 0, no. 0, pp. 0–0, 2023, doi: 10.21608/jesaun.2023.177464.1184.

[9] D. S. Simulia, “Abaqus 6.14 / Analysis User’s Guide,” *ABAQUS 6.14 Anal. User’s Guid.*, vol. I, p. 862, 2014.

[10] M. F. Hassanein and O. F. Kharoob, “Shear buckling behavior of tapered bridge girders with steel corrugated webs,” *Eng. Struct.*, vol. 74, pp. 157–169, 2014, doi: 10.1016/j.engstruct.2014.05.021.

[11] A. Bedynek, E. Real, and E. Mirambell, “Tapered plate girders under shear: Tests and numerical research,” *Eng. Struct.*, vol. 46, pp. 350–358, Jan. 2013, doi: 10.1016/j.engstruct.2012.07.023.

[12] J. G. Nie, L. Zhu, M. X. Tao, and L. Tang, “Shear strength of trapezoidal corrugated steel webs,” *J. Constr. Steel Res.*, vol. 85, pp. 105–115, 2013, doi: 10.1016/j.jcsr.2013.02.012.

[13] M. F. Hassanein and O. F. Kharoob, “Behavior of bridge girders with corrugated webs: (II) Shear strength and design,” *Eng. Struct.*, vol. 57, pp. 544–553, 2013, doi: 10.1016/j.engstruct.2013.04.015.

[14] L. S. da Silva, R. Simões, and H. Gervásio, “Eurocode 3: Part 1-1: General rules and rules for buildings,” vol. 3, no. 1, 2010, [Online]. Available: http://doi.wiley.com/10.1002/9783433601099

[15] J. Moon, J. Yi, B. H. Choi, and H. E. Lee, “Shear strength and design of trapezoidally corrugated steel webs,” *J. Constr. Steel Res.*, vol. 65, no. 5, pp. 1198–1205, 2009, doi: 10.1016/j.jcsr.2008.07.018.

[16] R. Sause and T. N. Braxtan, “Shear strength of trapezoidal corrugated steel webs,” *J. Constr. Steel Res.*, vol. 67, no. 2, pp. 223–236, 2011, doi: 10.1016/j.jcsr.2010.08.004.

Nomenclature

a	The span's length (mm)
b	Horizontal fold width (mm)
c	The width of the angled fold (mm)
D_x	Measurement of transverse bending stiffness for the inclined fold of the corrugated web per unit length. (mm)
Dy	The longitudinal bending rigidity per unit length of the corrugated web (mm)
E	Young's modulus of elasticity for steel (MPa)
f_y	The yield strength of the steel material. (MPa)
f_u	Maximum load capacity of the steel. (MPa)
h_w	Depth of the Web (mm)
h_{wo}	The tapered corrugated web's minimum depth (mm)
h_r	Corrugation cross-section depth (mm)
I_y	The corrugated web's moment of inertia (mm^4)
k_G	Coefficient of global shear buckling.
k_L	Coefficient of local shear buckling.
n	Interactive buckling capacity sequence.
q	Length of a single corrugation wave in horizontal projection. (mm)
w	The maximum fold width of both the inclined c and flat panels b (mm)
Θ	The angle of inclination of the sloped fold.
α	The angle of inclination of either the upper or lower flange of the tapered girder.
λ_s	The parameter associated with shear buckling in corrugated web structures.
τ_{cr}	Stress from critical shear buckling (MPa)
$\tau_{cr}.L$	Buckling stress at the local critical shear (MPa)
$\tau_{cr}.G$	Buckling stress at the Global critical shear (MPa)
$\tau_{cr.FE}$	FE Stress from critical shear buckling (MPa)
$\tau_{cr}.I$	Buckling stress at the Interactive critical shear (MPa)
P_{u-FEM}	FE local ultimate shear force (kN)
P_{u-Prp}	Proposed local ultimate shear force (kN)
τ_y	Shear yield strength of the steel (MPa)
ν	The Poisson's ratio of steel.